BULLETIN OF THE POLISH ACADEMY OF SCIENCES
TECHNICAL SCIENCES
DOI: 10.24425/bpasts.2024.150335

Robust Control of Motion in Presence of Uncertain Parameters and Control Constraints

Marcin Jastrzębski, Jacek Kabziński, Przemysław Mosiołek

Lodz University of Technology. Institute of Automatic Control

Abstract. The paper describes a novel, simple servo drive position controller, using only knowledge about the structure of the nonlinear model and the constraints met by individual components of the model. The desired behaviour of the position and velocity signals is obtained by imposing a time-varying constraint on the signal aggregating information about position and velocity tracking errors. The method allows you to determine the maximum control (servo drive current) necessary to achieve the control goal under the existing initial conditions and the selected reference trajectory. The control is constrained and consists in appropriate reaction when the trajectory approaches the barrier, the shape of which is responsible for the imposed properties of the transient and quasi-steady state tracking error. In addition to the derivation of the control, a discussion of its possible variants and basic properties is presented. Control with time-varying constraints has been introduced, which allows the control objectives to be met with limited conservatism of the imposed constraints. The influence of technical factors related to actual speed and position measurements was discussed and the operation of the real drive on a laboratory stand was presented.

Key words: nonlinear control, servo control, robust control

1. INTRODUCTION

The problem of ensuring appropriate properties of the control system in transient states and maintaining various constraints has been one of the key issues in control theory for decades. Its main difficulty is that, except for very simple linear systems, the relationship between the parameters the controller and the properties of the closed system in the transition state is complicated and no analytical models are known. Typically, control systems are designed to assure closed loop system stability, with appropriate stability margins, while the remaining features, such as a proper transient and satisfying constraints on state and control variables are provided additionally, within the existing freedom in parameter tuning. For instance, a PID controller can be automatically tuned to obtain a given overshoot value, minimize the appropriate integral performance index, and work correctly with the control signal saturation, but this will not guarantee compliance with the requirements and limitations in the case of each reference signal or each disturbance from a given class, especially in the case of a non-linear plant.

In recent years, several control methods have been developed to ensure appropriate transient behaviour, also in the case of nonlinear systems. Some of these are:

- Finite-time stability (FTS) and control [1], [2], [3], [4], [5], [6]. It provides stabilization for a given duration of the transient process (in some solutions freely set by the designer), uses Lyapunov methods and adaptive control techniques, usually does not take into account control constraints and requires access to state variables.
- Model reference adaptive control (MRAC) [7], [8]. It involves adaptive adjusting the response of the control system to the response of the model. Initially (1990s) used for linear or affine systems. Developed to ensure the robustness of the adaptive system, especially to disturbances, and to speed up the response.
- Prescribed performance control (PPC) [9], [10], [11]. It ensures that the tracking error converges to a predetermined set, with an imposed convergence decrement. This is achieved by transforming the initial constrained system into an unconstrained one such that its stability implies satisfaction of the constraints in the original system. Taking into account control constraints and delays may be an issue.
- Funnel control (FC) and polyhedral tubes control (PTC) [12], [13], [14], [15], [16]. It ensures that for a given class of signals the tracking error remains in a ‘funnel’ defined by specifying its nonlinear ‘generator’. PTC uses a conversion from a set of response parameters to a polyhedral set of state space constraints. It is a combination of numerical and analytical methods.

Ensuring appropriate transient of position and velocity is the basic problem of servo drive control. The basic aims of servo drive position control are to ensure adequate tracking accuracy of the reference trajectory in the quasi-steady state, obtain appropriate transient dynamics and meet the constraints imposed on state variables and control signals. These requirements should be absolutely met despite: unknown or changing parameters of the drive model, non-linear, not

precisely known friction, disturbances occurring during drive operation, unmodelled dynamics of the real plant.

Approaches that have been used to control servo drives include, for example, the use of: various variants of sliding-mode control [17], [18], a fuzzy controller tuning system [19], barrier Lyapunov functions [20], nonlinear transformation of state variables [21], a robust observer cooperating with a nonlinear adaptive controller [22], time-dependent Lyapunov barrier functions [23], and others. All of them are based on the plant model and its parameterization, although the parameters do not have to be known precisely. Some (e.g. methods using barrier Lyapunov functions) require testing and meeting complicated feasibility conditions. All of them lead to quite complex controllers containing nonlinear control laws, numerous adaptation laws and several tuning parameters.

In this contribution we propose a novel, simple servo drive position controller, using only knowledge about the structure of the nonlinear model and the constraints met by individual components of the model. The desired behaviour of the position and velocity signals is obtained by imposing a time-varying constraint on the signal aggregating information about position and velocity tracking errors. The method allows you to determine the maximum control (servo drive current) necessary to achieve the control goal under the existing initial conditions and the selected reference trajectory. The control is constrained and consists in appropriate reaction when the trajectory approaches the barrier, the shape of which is responsible for the imposed properties of the transient and quasi-steady state tracking error.

In addition to the derivation of the control, a discussion of its possible variants and basic properties is presented. Control with time-varying constraints has been introduced, which allows the control objectives to be met with limited conservatism of the imposed constraints. The influence of technical factors related to actual speed and position measurements was discussed and the operation of the real drive on a laboratory stand was presented.

2. PLANT MODEL AND CONTROL AIM

We consider a general model of motion with unknown parameters:

$$\begin{aligned} \dot{x}_1 &= x_2, \\ J\dot{x}_2 &= f(x,p) - \gamma(x,q) + g(x)u + d, \end{aligned} \tag{1}$$

where:

- the state variables $x = [x_1, x_2]^T$ represent position and velocity of a rigid body,
- J stands for the body inertia,
- $f(x,p)$ represents parameterized model of any external torques, for instance friction or any forces related to contact with the environment, depending on unknown parameters p, and acting against the motion,
- $\gamma(x,q)$ denotes a model of external torques, parameterized by unknown parameters q; these torques, e.g. resulting from gravity or springiness, may support or counteract the motion, depending on the direction of movement,
- d stands for an unstructured (being unknown function of state variables and time) disturbance or modeling errors; the sign of this component is unknown,
- $g(x)$ is an actuator gain,
- u stands for the control input, the desired propelling force or torque, or any other variable corresponding to the actual propelling torque or force, for instance the desired current of the motor forcing the motion.

Schematic diagrams of exemplary plants corresponding to the proposed model are presented in Fig. 1 and 2. Although the presented notation is typical for rotational motion, it can be used to describe linear motion as well.

We assume that the sign and the constraints of the actuator gain are known:

$$0 < g_m \le g(x) \le g_M. \tag{2}$$

We suppose that the inertia is constrained

$$0 < J_m \le J \le J_M \tag{3}$$

and that the unstructured disturbance fulfils

$$|d(t)| \le D. \tag{4}$$

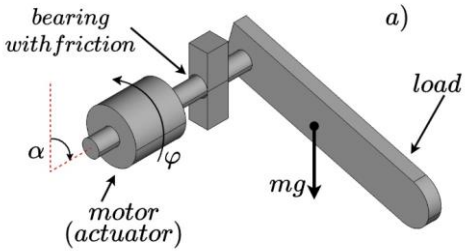

Fig.1. Diagram of an exemplary drive corresponding to the proposed model: a motor moving an arm in presence of gravity.

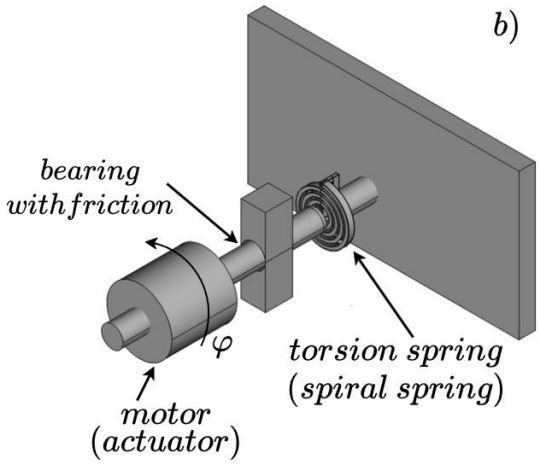

Fig.2. Diagram of an exemplary drive corresponding to the proposed model: a motor working against a torsion spring.

As the sign of $d(t)$ is unknown, it is impossible to use this information in the control loop, although a specific sign of the disturbance can work for or against the system stability.
It is also assumed that parameters p belong to a compact set P, the parameters q belong to a compact set Q, and that for any constrained set S of state variables, knowing the constraints for plant parameters, it is possible to calculate such $F_S > 0$ and $\gamma_S > 0$ that

$$\forall_{x\in S}: \forall_{q\in Q} |\gamma(x,q)| \le \gamma_S,\ \forall_{p\in P} |f(x,p)| \le F_S. \qquad (5)$$

The constrains presented in inequalities (2-5) constitute the only information about the plant which can be used to design the controller. Neither specific information about the functions $f(x,p), g(x), \gamma(x,q)$ nor about the disturbance $d(t)$ is necessary.
The control aim is to follow a smooth, bounded desired position trajectory $x_{1d}(t)$. It is assumed that the velocity and the acceleration defined by the desired position trajectory are also bounded:

$$|x_{1d}(t)| \le A_0, |\dot{x}_{1d}(t)| \le A_1, |\ddot{x}_{1d}(t)| \le A_2. \qquad (6)$$

The control aim is achieved if the tracking error

$$e_1 = x_1 - x_{1d} \qquad (7)$$

fulfils the implication:
For given positive design parameters $\alpha, \alpha_\infty, \mu$, if:

$$|e_1(0)| \le \alpha + \alpha_\infty = \alpha_0 \qquad (8)$$

then

$$\forall_{t>0}\ |e_1(t)| \le \alpha e^{-\mu t} + \alpha_\infty = A(t). \qquad (9)$$

The design parameter α_∞ represents the steady-state tracking accuracy, α_0 describes the initial state, and μ decides about the transient to a steady-state.
Therefore, any trajectory inside the constraints (9) is accepted.
The control aim must be achieved by a bounded control

$$\forall_{t>0}\ |u(t)| \le U \qquad (10)$$

and the constraint U must be derived as a function of design parameters $\alpha, \alpha_\infty, \mu$.

3. EXTENDED TRACKING ERROR

Let us select another design parameter $\lambda > \mu$ and define the extended tracking error:

$$r(t) = \lambda e_1(t) + \dot{e}_1(t). \qquad (11)$$

The extended tracking error allows to control both state variables of motion – position and velocity. The tracking error $e_1(t)$ can be considered as an output of the inertial filter with a transfer function

$$G(s) = \frac{1}{s+\lambda} \qquad (12)$$

excited by the extended tracking error $r(t)$. Therefore, the tracking error and the extended tracking error are directly related, and the insight into this relation in the context of constrains (9) is described by the lemma 1.
Lemma 1
Assume that the initial constraint (8) is satisfied, that the extended tracking error fulfils

$$|r(t)| \le \alpha_r e^{-\mu t} + \alpha_{r\infty} = A_r(t), \qquad (13)$$

and that

$$\alpha = \frac{\alpha_r}{\lambda-\mu},\ \alpha_\infty = \frac{\alpha_{r\infty}}{\lambda}. \qquad (14)$$

Then:
1) the tracking error fulfils the constraint (9),
2) the derivative of the tracking error is bounded:

$$\begin{aligned} |\dot{e}_1(t)| \le B(t) &= \alpha_r \left(1 + \frac{\lambda}{\lambda-\mu}\right) e^{-\mu t} + 2\alpha_{r\infty} \\ &= (2\lambda - \mu)\alpha e^{-\mu t} + 2\lambda\alpha_\infty. \end{aligned} \qquad (15)$$

The proof is given in the Appendix.
Hence, if we are able to control the extended tracking error in such a way that condition (13) is satisfied and the parameters are selected according to equations (14), then the control aim is achieved, and additionally the derivative of the tracking error is bounded according to Eq. (15). For the steady state (after several time constants $1/\mu$), the tracking error is bounded by $\alpha_\infty = \alpha_{r\infty}/\lambda$ and its derivative by $2\alpha_{r\infty}$.

4. CONTROL OF EXTENDED TRACKING ERROR

4.1. Violation of constraints.

Suppose that in a certain time interval $0 \le t < t_1$ the extended tracking error trajectory remains inside the constraint (13), and that at $t < t_1$ it is crossing the constraint. Therefore, two cases are possible.
Case 1:
The extended tracking error $r(t)$ crosses the upper (positive) constraint $A_r(t)$, so $r(t) - A_r(t)$ increases to zero left-side:

$$r(t) - A_r(t) \underset{t\to t_1}{\nearrow} 0^- . \qquad (16)$$

Therefore, for a certain δ, for any $t_1 - \delta < t \le t_1$ we have

$$\dot{r}(t) - \dot{A}_r(t) > 0 \Rightarrow \dot{r}(t) > -\mu\alpha_r e^{-\mu t} \qquad (17)$$

and, in particular, the inequality

$$\dot{r}(t_1) > -\mu\alpha_r e^{-\mu t_1} > -\mu\alpha_r \qquad (18)$$

is a necessary condition for crossing the constraint.

Case 2:
The extended tracking error $r(t)$ crosses the lower (negative) constraint $-A_r(t)$, so $r(t) - A_r(t)$ decreases to zero right-side:

$$r(t) + A_r(t) \underset{t\to t_1}{\searrow} 0^+. \tag{19}$$

Therefore, for a certain δ, for any $t_1 - \delta < t \le t_1$ we have

$$\dot{r}(t) + \dot{A}_r(t) < 0 \Rightarrow \dot{r}(t) < \mu\alpha_r e^{-\mu t} \tag{20}$$

and, in particular, the inequality

$$\dot{r}(t_1) < \mu\alpha_r e^{-\mu t_1} < \mu\alpha_r \tag{21}$$

is a necessary condition for crossing the constraint.
In conclusion, if the control strategy prevents fulfilling conditions (18) and (21), the extended tracking error remains inside constraints (13).

4.2. Derivation of the controller.

Behaviour of the extended tracking error is described by the equation:

$$\dot{r} = \lambda\dot{e}_1 + \ddot{e}_1 = \lambda\dot{e}_1(t) + \ddot{x}_1 - \ddot{x}_{1d}. \tag{22}$$

Hence, using equation (1) to substitute $\ddot{x}_1 = \dot{x}_2$ we obtain

$$\dot{r} = \lambda\dot{e}_1 - \frac{1}{J}\gamma + \frac{1}{J}f + \frac{1}{J}gu + \frac{1}{J}d - \ddot{x}_{1d}. \tag{23}$$

Let us assume that for $t < t_1$ $r(t)$ remains inside the constraints (13) (hence, $e_1(t)$ fulfils Eq. (9)) and consider components $\lambda\dot{e}_1(t)$, $f(x(t),p)$, $\gamma(x(t),q)$, $g(x(t))$, $d(t)$, $\ddot{x}_{1d}(t)$, which appear in equation (23). Each of them is bounded and the constraints can be calculated and denoted as follows:

1) Because of Eq. (15)

$$\lambda|\dot{e}_1(t)| \le \lambda\alpha_r\left(1 + \frac{\lambda}{\lambda-\mu}\right) + 2\lambda\alpha_{r\infty} =: E. \tag{24}$$

2) The state variables $x_1(t) = x_{1d}(t) + e_1(t)$, $x_2(t) = \dot{x}_{1d}(t) + \dot{e}_1(t)$ remain inside a compact set S because of Eq. (6), (9) and (15). Therefore, according to Eq. (5):

$$\begin{aligned} |f(x(t),p)| &\le F_S \\ |\gamma(x(t),q)| &\le \gamma_S. \end{aligned} \tag{25}$$

3) The constraints for $g(x(t))$, $d(t)$, $\ddot{x}_{1d}(t)$ are already defined in Eq. (2), (4) and (5).

Let us consider any smooth, constrained control $u(t)$, depending on $r(t)$ and $A_r(t)$, fulfilling three conditions:

$$|u(t)| \le U, \tag{26}$$

$$r(t) - A_r(t) \underset{t\to t_1}{\nearrow} 0^- \Rightarrow u(t) \underset{t\to t_1}{\longrightarrow} -U, \tag{27}$$

$$r(t) + A_r(t) \underset{t\to t_1}{\searrow} 0^+ \Rightarrow u(t) \underset{t\to t_1}{\longrightarrow} U. \tag{28}$$

Consider case 1 when $r(t) - A_r(t) \underset{t\to t_1}{\nearrow} 0^-$. It follows from Eq. (23) and (27), (25-26), (2), (4) and (6) that

$$\lim_{t\to t_1}\dot{r}(t) \le \lambda\dot{e}_1 + \frac{1}{J}\gamma_s + \frac{1}{J}F_s - \frac{1}{J}gU + \frac{1}{J}D + A_2. \tag{29}$$

If

$$U \ge \frac{1}{g_m}\{J_M(E + \mu\alpha_r + A_2) + \gamma_s + F_S + D\} \tag{30}$$

then

$$J(E + \mu\alpha_r + A_2) + \gamma_s + F_S + D < g_m U \tag{31}$$

and, from Eq. (29),

$$\lim_{t\to t_1}\dot{r}(t) \le -\mu\alpha_r. \tag{32}$$

As Eq. (32) contradicts Eq. (18), violation of constraints as described in case 1 is impossible.
Considering case 2, when $r(t) + A_r(t) \underset{t\to t_1}{\searrow} 0^+$, we have, from Eq. (23) and (28), (25-26), (2), (4) and (6) that

$$\lim_{t\to t_1}\dot{r}(t) \ge -E - \frac{1}{J}\gamma_s - \frac{1}{J}F_S + \frac{1}{J}g_m U - \frac{1}{J}D - A_2 \tag{33}$$

and, because of Eq. (31),

$$\lim_{t\to t_1}\dot{r}(t) \ge \mu\alpha_r. \tag{34}$$

As Eq. (34) contradicts Eq. (21), violation of constraints as described in case 2 is impossible.
In conclusion: any control law satisfying conditions (26-28) and (30) assures that the tracking error which satisfies the initial condition (8) remains inside the constraints (9) and therefore the control aim is achieved.

4.3. Variants of the control law.

Conditions (26-28) defining the control leave a lot of freedom in shaping the control when the extended error remains inside the constraints. Several smooth functions can be used. For instance, functions:

$$u(t) = -\frac{2U}{\pi}\arctan\left(K\tan\left[\frac{\pi}{2}sat_{1-\varepsilon}\left(\frac{r(t)}{A_r(t)}\right)\right]\right), \tag{35}$$

or

$$u(t) = -U\tanh\left(K\,\mathrm{atanh}\left[sat_{1-\varepsilon}\left(\frac{r(t)}{A_r(t)}\right)\right]\right) \tag{36}$$

where $sat_{1-\varepsilon}(*)$ denotes saturation to the range $[-1+\varepsilon, 1-\varepsilon]$, $\varepsilon \to 0$ fulfil conditions (26-28) and parameter K can be used to shape the control inside the constraints. The input $r(t)$ comes

from measurement and includes the measured velocity, so the function $sat_{1-\varepsilon}(*)$ preserves the correct operation of the drive in case of outliers.

In addition to the parameters describing the shape of $u(t)$ (as K in Eq. (35-36)), an important design parameter is $\lambda > 0$ used in Eq. (11) to define $r(t)$. Increasing λ decreases the participation of velocity in the extended error $r(t)$, decreases the quasi-steady-state error α_∞, but also increases the required control (see Eq. (24) and (30)). All parameters must be tuned and optimized taking into account the trajectory of the tracking error and the consumption of energy required to keep the tracking error inside the constraints.

Finally, we obtain a smooth control which is easy to implement, as the constraints $\pm U$ are constant during the system operation. Moreover, this control will be effective:

- for any plant satisfying the constraints (2-5),
- for any reference trajectory meeting assumption (6),
- for any initial conditions satisfying constraints (8) and (13).

On the other hand, the control law (26-28), (30) is rather conservative. This conclusion follows from the fact that the constraints appearing in Eq. (30) can be created with large security margins and from the fact that particular components of the right side of equation (23) are constrained separately and finally, the sum of constraints is applied. Typically, for a particular desired trajectory and initial conditions, the control aim can be achieved by a much smaller control constraint U then this given in Eq. (30).

Inspection of the extended error derivative Eq. (23) leads to conclusion that certain components of Eq. (23) can be measured (as $\lambda\dot{e}_1$), known in advance (like $\ddot{x}_{1d}(t)$) or constrained more precisely by time-varying bounds. Moreover, constraining some components of Eq. (23) together, rather than separately can provide more effective time-varying control. For instance:

1) For a given t the state variables $x_1(t) = x_{1d}(t) + e_1(t)$, $x_2(t) = \dot{x}_{1d}(t) + \dot{e}_1(t)$ remain inside a compact set $S(t)$ because of Eq. (6), (9) and (15). Therefore, according to Eq. (5):

$$|f(x(t), p)| \le F_S(t) \tag{37}$$

2) Moreover, as torque $\gamma(x(t), q)$ can support the desired motion, it can be more effective to constrain components $\gamma(x(t), q)$ and $J\ddot{x}_{1d}(t)$ together. Therefore, because of Eq. (5) and (6) there exists such bounded $\gamma_1(t)$ that:

$$|\gamma(x(t), q) + J\ddot{x}_{1d}(t)| \le \gamma_1(t) \tag{38}$$

3) Similarly, deeper analysis of the disturbance can provide us with tighter constraints

$$|d(t)| \le D(t). \tag{39}$$

Also, inequalities (18) and (21) provide time-varying necessary conditions for crossing the limits by $r(t)$.

Taking all these observations into account, a tiny modification of the derivation presented in section 4.2 provides a variant of the control law with time-varying extremum control values:

$$|u(t)| \le U(t), \tag{40}$$

$$r(t) - A_r(t) \underset{t\to t_1}{\nearrow} 0^- \Rightarrow u(t) \underset{t\to t_1}{\longrightarrow} -U(t_1), \tag{41}$$

$$r(t) + A_r(t) \underset{t\to t_1}{\searrow} 0^+ \Rightarrow u(t) \underset{t\to t_1}{\longrightarrow} U(t_1). \tag{42}$$

$$U(t) \ge \frac{1}{g_m}\{J_M(|\lambda\dot{e}_1(t)| + \mu\alpha_r e^{-\mu t}) + \gamma_1(t) + F_S(t) + D(t)\} \tag{43}$$

Finally, the control is given by Eq. (35) or (36) where U is substituted by $U(t)$.

The inequality (43) is not the only possible constraint of the control. Connecting other components of Eq. (23) and making use of a particular knowledge about the system can provide another, specific bounds.

The smoothness of the control constraint $U(t)$ can also effect the drive performance. Avoiding rapid current changes is an important factor influencing the drive behaviour and reliability. Therefore, instead of using the strict constraint (43), it can be recommended to use sufficiently smooth $U(t)$ fulfilling the inequality (43).

The other concept of control strategy is to apply extremal values of control not only if the extended tracking error reaches the constraint, by also if it is inside the constraints, for instant:

$$u(t) = \begin{cases} -U(t) \ \ if \ \ 0 \le r(t) \le A_r(t) \\ U(t) \ \ if \ \ -A_r(t) \le r(t) \le 0' \end{cases} \tag{44}$$

Unfortunately, this results in chattering, and therefore can be applied in particular applications only.

5. EXPERIMENTS

Simulation and real drive experiments are performed using the plant presented in Fig. 3. A permanent magnet synchronous motor AKM2G-41-PL, manufactured by Kollmorgen, is connected with a massive arm pointing to the ground and perpendicular to the motor axis. The control system is implemented using a PWM inverter Kolmorgen AKD-T02406 with the current controller on board. The complete control algorithm is implemented on dSPACE MicroLabBox programmed from Simulink. Data acquisition is done by ControlDesk software.

The drive is modelled by equation (1), where

- the torque $f(x, p)$ acting against the motion is composed of the static and viscous friction given by $f(x, p) = -p_1 \tanh(100x_2) - p_2 x_2$ (p_1 is a static friction coefficient and p_2 is a viscous friction parameter);
- the torque $\gamma(x, q)$ originates from gravity, it acts against the motion if the arm is raised and it helps the motion

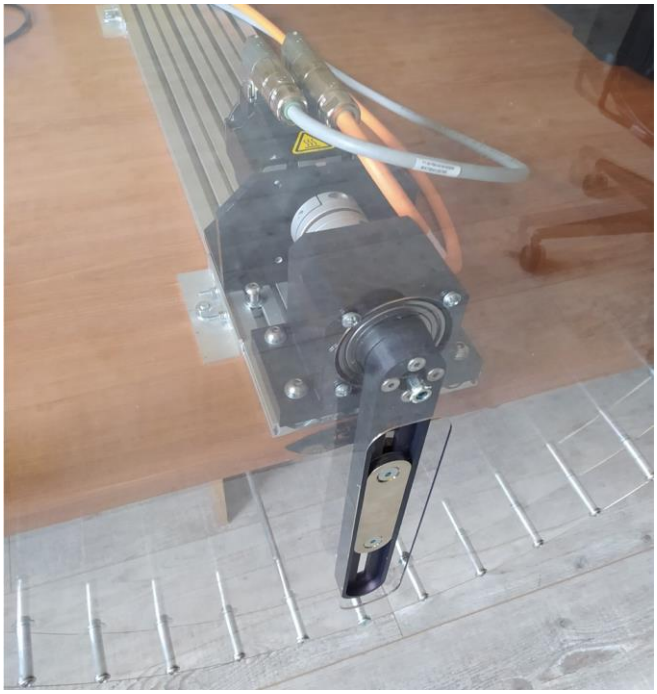

Fig.3. The servo system

when the arm moves down and is given by $\gamma(x, q) = q\sin(x_1)$;

- the torque/current coefficient $g(x)$ is usually constant, although it can vary with the rotor position in case of some motor construction irregularities;
- u denotes the desired current value – the current control loop reference; as it will be demonstrated, the dynamics of this loop can be neglected and therefore u approximates the actual current;
- d denotes a disturbance representing all modelling errors, omitted current dynamics, not included nonlinearities, etc.
- position $x_1 = 0$ means that the arm points down and clock-wise direction is positive.

The estimation of the drive parameters was based on the motor nominal data and some experiments performed earlier. All these allows to find reliable upper and lower bounds for the model parameters and the disturbance presented in Table 1.

The ideal model of the plant was constructed using middle values of parameters presented in Table 1.

TABLE 1. SERVO PARAMETERS

		lower constr.	*upper constr.*
$J\ [kgm^2]$	moment of inertia	$J_m = 0.0239$	$J_M = 0.0292$
$g\ [Nm/A]$	torque/current constant	$g_m = 0.1323$	$g_M = 0.1455$
$\lvert d\rvert\ [Nm]$	disturbance	0	$D = 0.1$
$p_1\ [Nm]$	static friction parameter	$p_{1m} = 0.0203$	$p_{1M} = 0.0377$
$p_2\ [Nms/rad]$	viscous friction parameter	$p_{2m} = 0.0041$	$p_{1M} = 0.0077$
$q\ [Nm]$	load coefficient	$q_m = 1.224$	$q_M = 1.496$

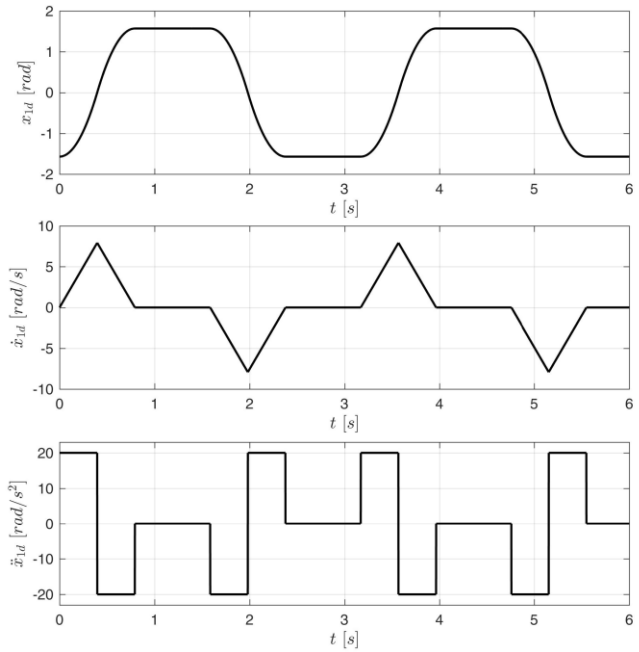

Fig.4. Desired trajectory

The time constant of the current control loop is estimated as 1 ms and was taken into account while building the model used for simulations.

The desired trajectory represents a swing movement between $\pm x_{1d}(0) = \pm\pi/2$ with stopping at extreme positions. It is depicted in Fig. 4.

The control aim is defined by constraints (9), or equivalently Eq. (13), with parameters: $\alpha_\infty = 1° = 0.0175\ [rad]$, $\mu = 3.5\ \left[\frac{1}{s}\right]$, $\alpha_0 = 5\,\alpha_\infty$. The steady-state constraint for the extended error $\alpha_{r\infty}$ is limited by a velocity measurement error, therefore $\alpha_{r\infty} = 0.25\ \left[\frac{rad}{s}\right]$ is selected, hence $\lambda = \frac{\alpha_{r\infty}}{\alpha_\infty} = 14.32\ \left[\frac{1}{s}\right]$. The constraints (9), (13) and (15) representing the control aim are plotted in Fig. 5.

Initial conditions during the experiments presented below are selected as $e_1(0) = 0.8\,\alpha_0,\ x_2(0) = 0$.

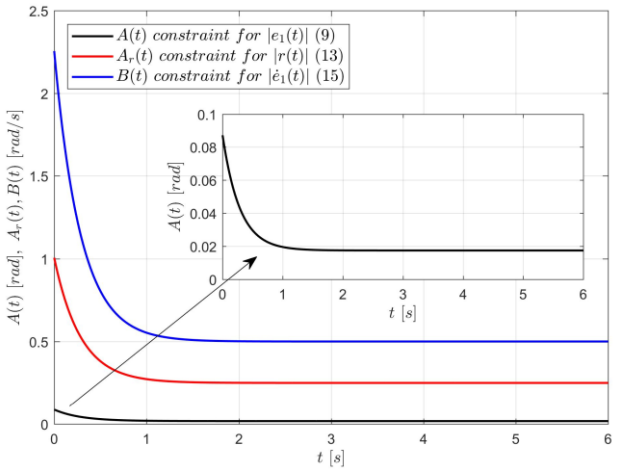

Fig.5. Constraints of $|\boldsymbol{e_1(t)}|, |\boldsymbol{r(t)}|, |\boldsymbol{\dot{e}_1(t)}|$

5.1. Constant control constraints

The desired position trajectory, constraints for model parameters and parameter λ enable calculation of all components necessary to obtain the control constraint U from inequality (30), where each component of the right side of Eq. (23) is constrained separatelly. The obtained values are presented in Table 2.

TABLE 2. CONSTRAINTS OF COMPONENTS IN INEQUALITY (30)

$J_M E/g_m$	$J_M \mu\alpha_r/g_m$	$J_M A_2/g_m$	γ_S/g_m	F_S/g_m	D/g_m
7.12	0.58	4.41	11.31	0.88	0.76

It follows from Eq. (30) that $U \geq 25\ [A]$ is necessary to achieve the control aim.

The function (36) with $K = 2$ was selected to construct the control.

The closed loop system was simulated for $U = 25\ [A]$ and the results are shown in Fig. 6. It is visible that, apart from a very short period, just after starting, the necssary current is far below the constraints imposed by a conservative condition (30). As a matter of fact, this contraol aim can be achieved with much smaller control, as it is demenstrated in Fig. 7 for $U = 10$.

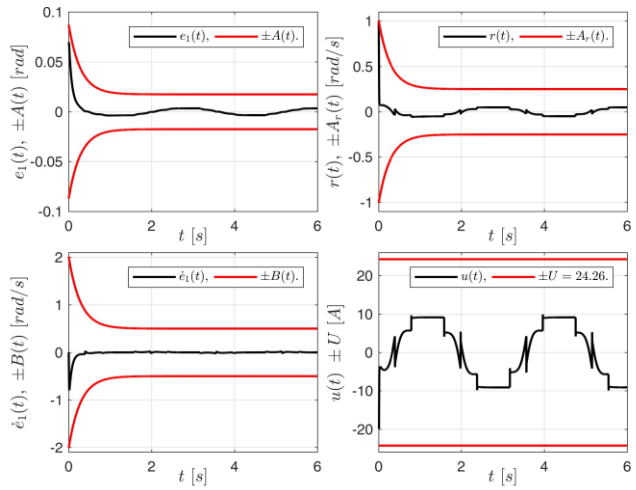

Fig.6. System performance for $\boldsymbol{U = 25\ [A]}$.

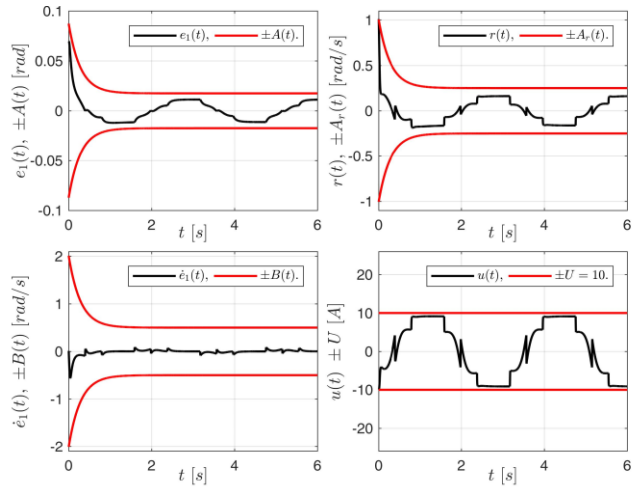

Fig.7. System performance for $\boldsymbol{U = 10\ [A]}$.

Although actual errors $|e_1(t)|$, and $r(t)$ are much closer to the constarints for smaller U, all tracking error constraints are stricly preserved.

5.2. Variable control constraints

Inequality (43) provides time-varying control constraints allowing to achieve the control aim. For the discussed drive, the particucal components of the right side of Eq. (43) are:

$$\begin{aligned} F_S(t) &= |p_{1M}\tanh(100x_2) + p_{2M}x_2|, \\ \gamma_1(t) &= \max_{(q,J)\in[q_m,q_M]\times[J_m J_M]} |qsin(x_1(t)) + J\ddot{x}_{1d}(t)|, \\ D(t) &= D, \end{aligned} \tag{45}$$

while $|\lambda\dot{e}_1(t)| + \mu\alpha_r e^{-\mu t}$ can be measured or calculated on-line.

The control given by Eq. (36) with $K = 2$, where U is substituted by

$$U(t) = \frac{1}{g_m}\{J_M(|\lambda\dot{e}_1(t)| + \mu\alpha_r e^{-\mu t}) + \gamma_1(t) + F_S(t) + D(t)\} \tag{46}$$

was applied. Results are demonstrated in Fig. 8.

The tracking quality is not worse then for $U = 25$ while the the control constraints are narrowed and much bettter siuitted to actual phase of motion. The fact that gravity helps the motion when the arm is mooving down is used to constrain the current effectivly.

5.3. Impact of measurement errors

To check the impact of factors connected with a real plant implementation, the operation of the arm position encoder was modelled with a resolution of $\delta = \frac{2\pi}{2^{13}}\ [rad]$ and the velocity was calculated as the backward difference from the encoder data. The sytem performane is presented in Fig.9.

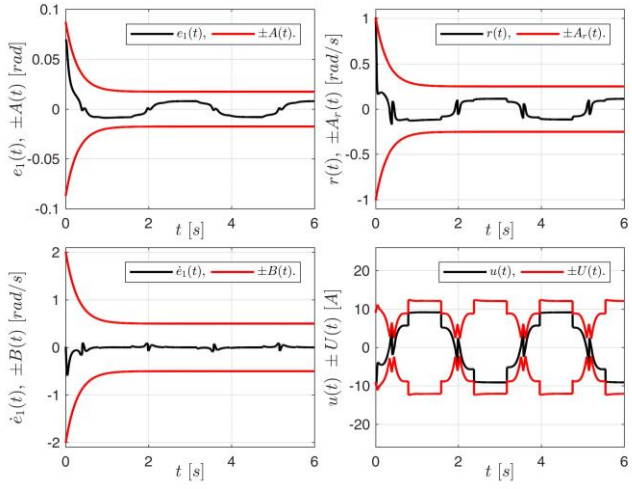

Fig.8. System performance for $\boldsymbol{U = U(t)}$.

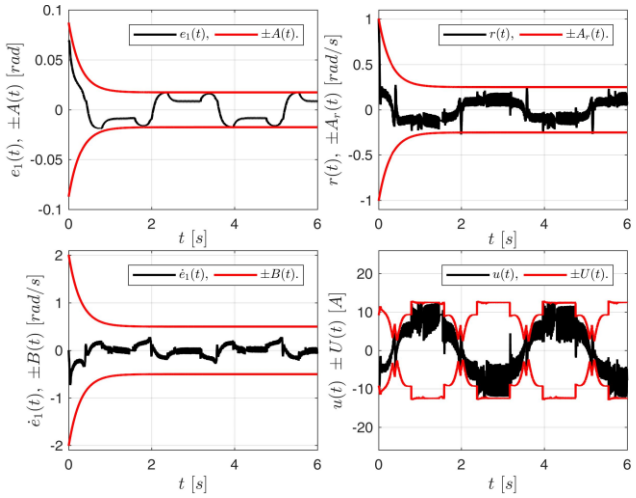

Fig.9. System performance for $\boldsymbol{U = U(t)}$ and inaccurate measurements.

Low accuracy of the calculated velocity and measurement noise significantly reduces the quality of control, but still the tracking errors are inside the constraints, so the control aim is achieved.

However, having in mind that the shape of the current is important for the drive reliability, we recomend using more suitable techniques for velocity measurement or calculations, providing smoother signal. This can be achieved using a simple linear observer based on a linearized model of the drive with average parametrs. The signals obtained from the conntrol system equiped with the velocity observer are plotted in Fig. 10.

5.4. Real drive experiments

Multiple experiments were performed with the real drive presented in Fig. 3. Results for the system with time-varying control constraint $U(t)$ given by Eq. (45-46) when $K = 2$ and velocity is provided by the observer are presented in Fig. 11. The system operates correctly, the control aim is achieved and the tracking error constraints are fulfilled with a sufficient margin. The actual motor current is very close to the desired current (blue line in Fig. 11, completely covered by the actual current plot – green line) and is safely placed inside the continuous current constraint $U_{max} = 19.9\ [A]$ provided by the motor manufacturer.

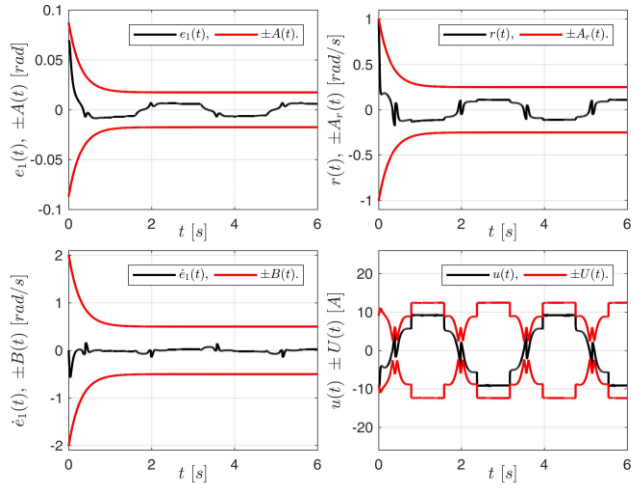

Fig.10. System performance for $\boldsymbol{U = U(t)}$ with the velocity observer.

The next experiments illustrate the impact of parameter K which changes the shape of the control functions (35) and (36). This is demonstrated in Fig. 12. Both functions, Eq. (35) and (36), can by formed similarly by a proper choice of K - see the black curves in Fig. 12. Small values of K result in small values of control inside the constraints and in a rapid increase of control close to the constraints. Higher K means that higher values of control are generated deeper inside the constraints $A_r(t)$.

Figure 13 illustrates the impact of K on real system performance in quasi-steady-state: $t > 35\mu^{-1} = 10s$. It is visible that small values of K should be avoided. Such small K causes high-frequency current oscillations and rapid transition of tracking errors in between the constraints. Increasing K from 2 to 10 decreases the tracking error, so acts similarly as decreasing α_∞, but without affecting the constraint $U(t)$, what α_∞, does. Higher values of K are ineffective in the presence of velocity measurement noise.

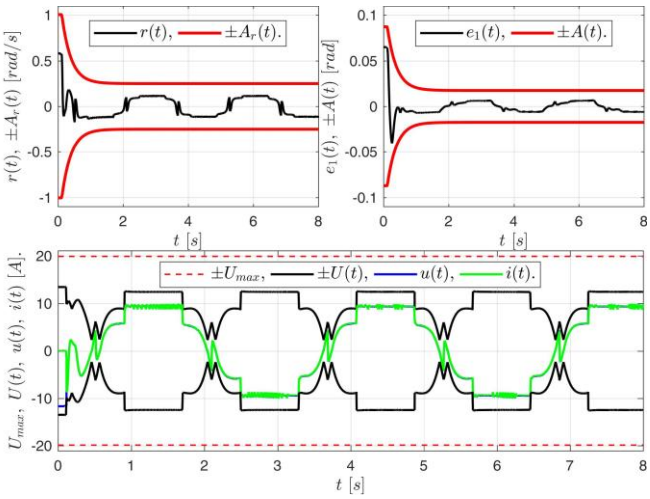

Fig.11. Real System performance for $\boldsymbol{U = U(t)}$ with the velocity observer.

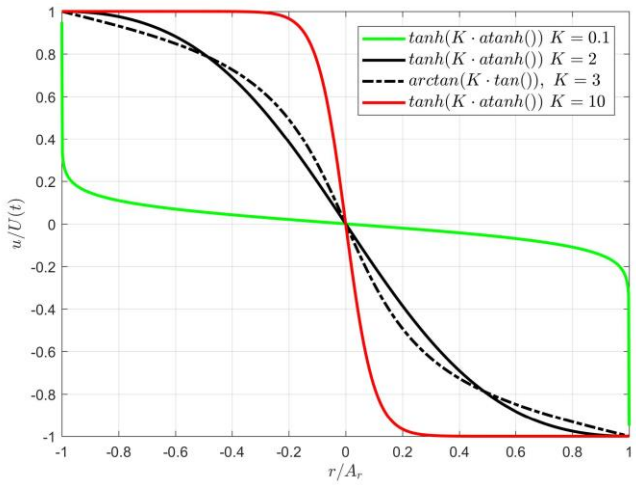

Fig.12. Shape of control functions (35), (36) for different values of parameter $\boldsymbol{K}$.

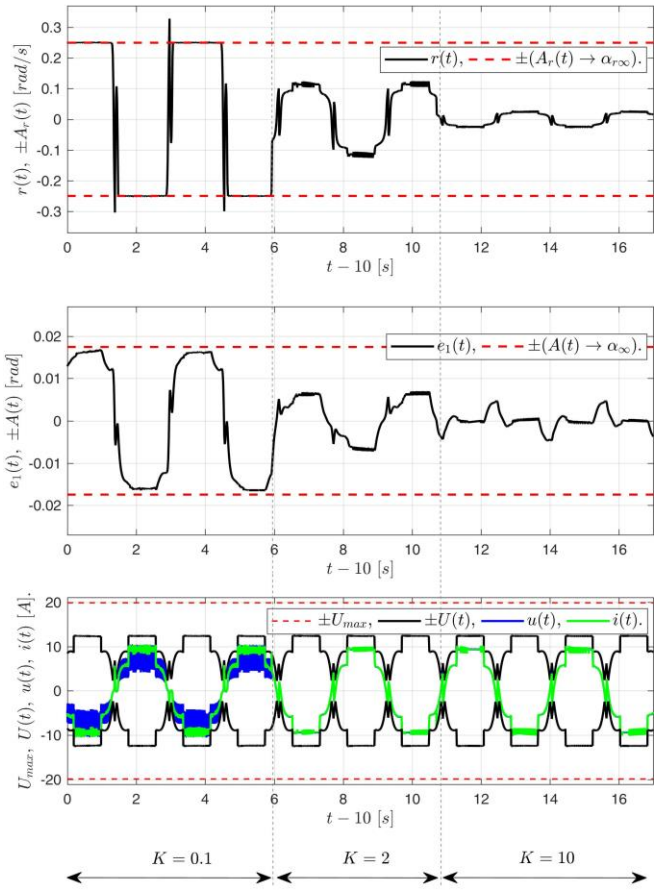

Fig.13. Quasi-steady-state performance of the real drive for different values of $\boldsymbol{K}$.

6. CONCLUSIONS

The presented method requires only approximate information about the servo model to achieve the control aim based on constraining the tracking error waveform during the transient and in a steady state. The parameters describing the control aim are simple and easily explainable. The presented approach makes it possible to determine the maximum control necessary to achieve the control aim under existing initial conditions and the selected reference trajectory. It was shown that these control constraints can be too conservative. In the presented approach it is described and recommended how to obtain and apply time-varying control constraints. The presented variants of control offer enough design flexibility to cope with various servos and reference trajectories. If more information about the system plant is available, it can be used to obtain more accurate constraints on model components and, finally, smaller values of the control. For instance information on the sign of the disturbance can be utilized this way.

The proposed control algorithm was implemented in a real system without any problems.

Although the control concerns a system with unknown parameters, the proposed approach does not use adaptive control methods, does not use Lyapunov methods to prove stability and uses knowledge about the plant model to a very limited extent.

The control does not use an integral controller, typical for servo systems. Therefore, there is no need to implement the integrator in the real system, which is often not trivial. One doesn't have to deal with the effects that occur when working on control saturation, which necessitates the use of special solutions (e.g. anti-windup) in the PI controller, limiting adaptive parameters in adaptive systems, or erasing errors of integrators after a failure, e.g. such as loss of power.

The proposed controller can be easily tuned during operation, and any incorrectly selected control parameters or measurement errors could be corrected online and did not require restarting the process. An incidental violation of tracking error constraints may occur when measurement errors (outliers) occur or when the maximum control value is too small. In any case the system is able to recover after correcting the situation on-line. The authors' research plans include investigation of auto-tunning of the proposed controller.

All the presented features, which prove the simplicity of implementation, support the great application possibilities of the proposed control method.

Servo systems are ubiquitous in modern industry and technology. Therefore, the discussed problem of precise and energy-saving servo control is of interdisciplinary nature and importance. The presented results remain within the broad scope of state-of-the-art motion control research [24], [25], [26] and offer a unique approach based solely on information about the constraints of the model components.

APPENDIX

Proof of Lemma 1.

Considering nonzero initial condition $e_1(0)$ and using equation (11) we get

$$|e_1(t)| = \left|\int_0^t e^{-\lambda(t-\tau)} r(\tau)d\tau + e_1(0)e^{-\lambda t}\right|. \quad \text{(A1)}$$

Next, using Eq. (13) and performing integration provides

$$|e_1(t)| \leq \frac{\alpha_r}{\lambda-\mu}\left(e^{-\mu t} - e^{-\lambda t}\right) + \frac{\alpha_{r\infty}}{\lambda}\left(1 - e^{-\lambda t}\right) + |e_1(0)|e^{-\lambda t}. \quad \text{(A2)}$$

Inequality (A2) can be re-arranged to get

$$|e_1(t)| \leq \frac{\alpha_r}{\lambda-\mu}e^{-\mu t} + \frac{\alpha_{r\infty}}{\lambda} + - \left(\frac{\alpha_r}{\lambda-\mu} + \frac{\alpha_{r\infty}}{\lambda} - |e_1(0)|\right)e^{-\lambda t}. \quad \text{(A3)}$$

Assuming Eq. (8) and (14) provides

$$|e_1(0)| \leq \frac{\alpha_r}{\lambda-\mu} + \frac{\alpha_{r\infty}}{\lambda} \quad \text{(A4)}$$

and it follows from Eq .(A3) that

$$|e_1(t)| \leq \frac{\alpha_r}{\lambda-\mu}e^{-\mu t} + \frac{\alpha_{r\infty}}{\lambda}. \quad \text{(A5)}$$

The bounds for the derivative $\dot{e}_1(t)$ follow from calculation:

$$|\dot{e}_1(t)| = |r(t) - \lambda e_1(t)| \leq \alpha_r e^{-\mu t} + \alpha_{r\infty} + \lambda\left(\frac{\alpha_r}{\lambda-\mu}e^{-\mu t} + \frac{\alpha_{r\infty}}{\lambda}\right) = \alpha_r\left(1 + \frac{\lambda}{\lambda-\mu}\right)e^{-\mu t} + 2\alpha_{r\infty} \quad \text{(A6)}$$
$$= (2\lambda - \mu)\alpha e^{-\mu t} + 2\lambda\alpha_\infty.$$

A short film presenting the drive during one of experiments is available at:
https://www.youtube.com/shorts/3bLE9HLvKV8

REFERENCES

[1] Q.-G. W. Junhui Zhang and J. Sun, "On finite-time stability of nonautonomous nonlinear systems," *Int J Control*, vol. 93, no. 4, pp. 783–787, 2020, doi: 10.1080/00207179.2018.1536831.

[2] X. Huang, W. Lin, and B. Yang, "Global finite-time stabilization of a class of uncertain nonlinear systems," *Automatica*, vol. 41, no. 5, pp. 881–888, 2005, doi: https://doi.org/10.1016/j.automatica.2004.11.036.

[3] S. Li, C. K. Ahn, and Z. Xiang, "Command-Filter-Based Adaptive Fuzzy Finite-Time Control for Switched Nonlinear Systems Using State-Dependent Switching Method," *IEEE Transactions on Fuzzy Systems*, vol. 29, no. 4, pp. 833–845, 2021, doi: 10.1109/TFUZZ.2020.2965917.

[4] H. Hou, X. Yu, L. Xu, K. Rsetam, and Z. Cao, "Finite-Time Continuous Terminal Sliding Mode Control of Servo Motor Systems," *IEEE Transactions on Industrial Electronics*, vol. 67, no. 7, pp. 5647–5656, 2020, doi: 10.1109/TIE.2019.2931517.

[5] B. Wang, M. Iwasaki, and J. Yu, "Finite-Time Command-Filtered Backstepping Control for Dual-Motor Servo Systems With LuGre Friction," *IEEE Trans Industr Inform*, vol. 19, no. 5, pp. 6376–6386, 2023, doi: 10.1109/TII.2022.3182341.

[6] K. Li and Y. Li, "Adaptive Neural Network Finite-Time Dynamic Surface Control for Nonlinear Systems," *IEEE Trans Neural Netw Learn Syst*, vol. 32, no. 12, pp. 5688–5697, 2021, doi: 10.1109/TNNLS.2020.3027335.

[7] J. Yang, J. Na, and G. Gao, "Robust model reference adaptive control for transient performance enhancement," *International Journal of Robust and Nonlinear Control*, vol. 30, no. 15, pp. 6207–6228, 2020, doi: https://doi.org/10.1002/rnc.5080.

[8] J. Na, G. Herrmann, and K. Zhang, "Improving transient performance of adaptive control via a modified reference model and novel adaptation," *International Journal of Robust and Nonlinear Control*, vol. 27, no. 8, pp. 1351–1372, 2017, doi: https://doi.org/10.1002/rnc.3636.

[9] S. Wang, "Nonlinear Uncertainty Estimator-Based Robust Control for PMSM Servo Mechanisms With Prescribed Performance," *IEEE Transactions on Transportation Electrification*, vol. 9, no. 2, pp. 2535–2543, 2023, doi: 10.1109/TTE.2022.3212671.

[10] J.-X. Zhang and G.-H. Yang, "Robust Adaptive Fault-Tolerant Control for a Class of Unknown Nonlinear Systems," *IEEE Transactions on Industrial Electronics*, vol. 64, no. 1, pp. 585–594, 2017, doi: 10.1109/TIE.2016.2595481.

[11] C. P. Bechlioulis and G. A. Rovithakis, "A low-complexity global approximation-free control scheme with prescribed performance for unknown pure feedback systems," *Automatica*, vol. 50, no. 4, pp. 1217–1226, 2014, doi: https://doi.org/10.1016/j.automatica.2014.02.020.

[12] W. Esterhuizen and Q.-G. Wang, "Finite-time stability and stabilisation with polyhedral domains for linear systems," *Int J Control*, vol. 93, no. 9, pp. 2086–2094, 2020, doi: 10.1080/00207179.2018.1541364.

[13] W. Esterhuizen and Q.-G. Wang, "Control design with guaranteed transient performance: An approach with polyhedral target tubes," *Automatica*, vol. 119, p. 109097, 2020, doi: https://doi.org/10.1016/j.automatica.2020.109097.

[14] Y. Cheng, X. Ren, D. Zheng, and L. Li, "Non-Linear Bandwidth Extended-State-Observer Based Non-Smooth Funnel Control for Motor-Drive Servo Systems," *IEEE Transactions on Industrial Electronics*, vol. 69, no. 6, pp. 6215–6224, 2022, doi: 10.1109/TIE.2021.3095811.

[15] A. Ilchmann, E. P. Ryan, and S. Trenn, "Tracking control: Performance funnels and prescribed transient behaviour," *Syst Control Lett*, vol. 54, no. 7, pp. 655–670, 2005, doi: https://doi.org/10.1016/j.sysconle.2004.11.005.

[16] A. Ilchmann, E. P. Ryan, and P. Townsend, "Tracking with Prescribed Transient Behavior for Nonlinear Systems of Known Relative Degree," *SIAM J Control Optim*, vol. 46, no. 1, pp. 210–230, 2007, doi: 10.1137/050641946.

[17] S. Brock, "Hybrid P–PI sliding mode position and speed controller for variable inertia drive," *Przegląd Elektrotechniczny*, vol. 5, pp. 29–34, 2014.

[18] S. Brock, "Sterowanie ślizgowe zapewniające zbieżność uchybu w skończonym czasie dla napędu bezpośredniego," *Przegląd Elektrotechniczny*, vol. 5, pp. 124–129, 2016.

[19] M. Żychlewicz, R. Stanisławski, J. Szrek, M. Malarczyk, and M. Kamiński, "Rozmyty regulator stanu układu dwumasowego," *Przegląd Elektrotechniczny*, vol. 3, pp. 53–58, 2023.

[20] J. Kabziński, P. Mosiołek, and M. Jastrzębski, "Adaptive position tracking with hard constraints—barrier lyapunov functions approach," in *Studies in Systems, Decision and Control*, vol. 75, Springer Berlin Heidelberg, 2017, pp. 27–52. doi: 10.1007/978-3-319-45735-2_2.

[21] J. Kabziński and P. Mosiołek, "Adaptive, nonlinear state transformation-based control of motion in presence of hard constraints," *Bulletin of the Polish Academy of Sciences: Technical Sciences DOI - 10.24425/bpasts.2020.134653*, vol. 68, no. No. 5 (i.a. Special Section on Modern control of

drives and power converters), pp. 963–971, 2020, doi: 10.24425/bpasts.2020.134653.

[22] J. Kabziński and P. Mosiołek, "Observer-Based, Robust Position Tracking in Two-Mass Drive System," *Energies (Basel)*, vol. 15, no. 23, 2022, doi: 10.3390/en15239093.

[23] M. Jastrzębski, J. Kabziński, and P. Mosiołek, "Finite-Time, Robust, and Adaptive Motion Control with State Constraints: Controller Derivation and Real Plant Experiments," *Energies (Basel)*, vol. 15, no. 3, 2022, doi: 10.3390/en15030934.

[24] Y. Cheng, X. Ren, D. Zheng, and L. Li, "Non-Linear Bandwidth Extended-State-Observer Based Non-Smooth Funnel Control for Motor-Drive Servo Systems," *IEEE Transactions on Industrial Electronics*, vol. 69, no. 6, pp. 6215–6224, 2022, doi: 10.1109/TIE.2021.3095811.

[25] Y. Su, C. Zheng, and P. Mercorelli, "Simple Saturated PID Control for Fast Transient of Motion Systems," *IFAC-PapersOnLine*, vol. 53, no. 2, pp. 8985–8990, 2020, doi: https://doi.org/10.1016/j.ifacol.2020.12.2013.

[26] H. Hou, X. Yu, L. Xu, K. Rsetam, and Z. Cao, "Finite-Time Continuous Terminal Sliding Mode Control of Servo Motor Systems," *IEEE Transactions on Industrial Electronics*, vol. 67, no. 7, pp. 5647–5656, 2020, doi: 10.1109/TIE.2019.2931517.